

Correlation between clinical, CT features and EGFR gene in minimally invasive adenocarcinoma

L.P. Zhou¹, L.M. Chang^{2*}, H. Zhao², X.Y. Yang², L.L. Shi³

¹Department of Function, The Fifth Hospital of Tangshan (CT/DR Room), Tangshan, China

²Department of Medical Imaging, Tangshan Gongren Hospital, Tangshan, China

³Department of Radiology, Tangshan Maternal and Child Health Hospital, Tangshan, China

ABSTRACT

► Original article

*Corresponding author:

L.M. Chang, M.D.,

E-mail: 240612799@qq.com

Received: March 2024

Final revised: April 2025

Accepted: April 2025

Int. J. Radiat. Res., January 2026;
24(1): 43-48

DOI: 10.61186/ijrr.24.1.7

Keywords: Lung adenocarcinoma, CT signs, epidermal growth factor receptor, tomography, X-ray computed.

Background: To analyze the correlation between epidermal growth factor receptor (EGFR) gene mutations and clinical as well as computed tomography (CT) signs in minimally invasive adenocarcinoma (MIA). **Materials and Methods:** A total of 118 patients with MIA treated at the Department of Thoracic Surgery, Tangshan Gongren Hospital, from December 2018 to December 2021 were included in this study. Patients were categorized into two groups based on their Epidermal Growth Factor Receptor (EGFR) mutation status: a mutation group and a wild-type group. Differences in clinical and CT features between the two groups were recorded and statistically analyzed. **Results:** Among the 118 patients, 69 were in the mutation group, while 49 were in the wild-type group. No significant differences were observed in gender, smoking history, age, mean nodule diameter, peripheral emphysema, air bronchogram, lobulation sign, pleural indentation sign, morphology, tumor-lung interface, peripheral fibrosis, and density between the two groups ($P > 0.05$). However, significant differences were noted in the spiculation sign, vacuole sign, and vascular convergence sign between the groups ($P < 0.05$). Logistic regression analysis identified the vacuole sign with an odds ratio (OR) of 0.410 ($P > 0.05$) and the spiculation sign and vascular convergence sign with ORs of 1.498 and 2.262, respectively ($P < 0.05$), as independent risk factors for predicting EGFR mutations. The areas under the ROC curves (AUC) for the spiculation sign and vascular convergence sign were 0.634 and 0.735, respectively, in distinguishing EGFR gene mutations in MIA. **Conclusion:** CT imaging demonstrated that MIA patients presenting with spiculation, vacuole, and vascular convergence signs had a higher likelihood of EGFR gene mutations. Among these, the spiculation and vascular convergence signs are critical, independent risk factors for predicting EGFR gene mutations in MIA patients.

INTRODUCTION

Lung cancer ranks second in about 18.4 percent of the causes of cancer deaths worldwide, according to the latest data ⁽¹⁾. In the pathological classification of NSCLC, adenocarcinoma has the highest incidence rate ⁽²⁾. With the rapid development of pathology and molecular biology, the study of lung adenocarcinoma has gradually deepened. The growth of lung adenocarcinoma follows the evolution pattern from in situ adenocarcinoma (AIS), MIA to gradually progressing to invasive adenocarcinoma (IAC) ^(3, 4). Different subtypes of lung adenocarcinoma subtypes need different surgical methods with different clinical outcomes ⁽⁵⁾. Therefore, accurate preoperative pathological type identification of lesions is crucial to the selection of surgical methods.

At present, most patients with lung adenocarcinoma have hidden clinical symptoms, and the pathological type of lesions cannot be determined when some lesions are detected. Due to a variety of reasons, patients cannot be treated surgically, mainly with radiotherapy and chemotherapy, but the side

effects of chemotherapy drugs cannot be tolerated by some patients, and the curative effect is not good ⁽⁶⁾.

With the continuous development of biological research, more and more scholars have transformed the traditional view of lung cancer treatment. The main clinical applications of biological therapy are also gradually becoming mature. Targeted drugs have major breakthroughs in the field of cancer, among which the EGFR epidermal growth factor receptor is the most studied and most documented molecular target compared with other driver genes ⁽⁷⁾. Studies show that is a critical receptor on the surface of various normal and mutant cells ⁽⁸⁾. As the EGFR gene decisive effect in promoting the growth and proliferation of tumor cells, increased levels of EGFR receptors can lead to disease progression and poor prognosis ⁽⁹⁾. Therefore, confirm the mutation status of EGFR is important for the molecular biological treatment lung adenocarcinoma because it allows the development of targeted therapeutic strategies to improve prognosis ⁽¹⁰⁾. Gefitinib is the most common targeted therapy drug, which not only has better therapeutic effect, but also has the advantages of oral

administration, good compliance and low toxicity⁽¹¹⁾. However, assessment targeting EGFR mutation status relies mainly on biopsy tissue. In practice, EGFR genetic testing poses challenges, especially because due to the high cost, many patients cannot afford the test and therefore cannot biopsy the tissue for molecular analysis. Moreover, there is obvious heterogeneity of tumor. The tumor tissue obtained by puncture cannot totally represent lesion, and duplicated puncture will increase the cost and secondary injury⁽¹²⁾. Although serum circulating tumor cell DNA (ctDNA) can be used as an addist method for congestion DNA testing, it is still impossible to accurately understand the EGFR gene mutation⁽¹³⁾. Accurate analysis of EGFR mutation status by invasive biopsy or ctDNA testing is sometimes not feasible. Therefore, researchers have been looking for more practical, cost-effective and straightforward approaches.

At present, CT, as the most commonly used test for lung cancer, is important in the diagnosis and efficacy evaluation of lung cancer. The biological behavior of the lesion determines its different growth patterns, and the differences in the growth patterns between the lesions can manifest by different imaging features⁽¹⁴⁾. This makes it possible to combine molecular biology with modern medical imaging, laying the theoretical foundation for molecular imaging. Imaging physicians are trying to indirectly obtain genetic mutation information from imaging features with lung cancer to help ensure driver genes. At present, there are many related studies in many directions and in the number, including more studies on morphology^(15, 16). Several studies have evaluated the characteristics of lung adenocarcinoma using computed tomography (CT) and concluded that CT signs can predict molecular subtypes based on genetic mutations⁽¹⁷⁾. However, these findings remain controversial⁽¹⁸⁾.

If we can apply CT to diagnose lesions early, and apply CT to extract multidimensional imaging features from the lesion area non-invasively analyze the tumor heterogeneity and find its internal connection with EGFR gene mutation, it can help clinical decision of treatment plan, choose surgery type or avoid unnecessary surgery. Most studies have focused on the general cases of invasive lung adenocarcinoma, which is highly innovative based on the study of clinical features, correlation of CT signs and EGFR gene mutations in this pathological type.

MATERIALS AND METHODS

Subjects

This study was approved by the Tangshan Gongren Hospital Ethics Committee (No. GRY-LL-2018-48). A retrospective analysis inducted 118 patients that underwent thoracic surgery at Tangshan Gongren Hospital between December 2018 and March 2021, all

of whom had been diagnosed with pathological minimally invasive adenocarcinoma (MIA). Each patient underwent a CT examination, and EGFR gene detection performed post-surgery. Among the 118 patients with MIA, 69 categorized into the mutant group, and 49 classified as the wild-type group. The cohort included 67 females and 51 males, aged 31 to 81 years. These cases further split into two teams, 60 years as the threshold: 48 patients were 60 years or younger, and 70 patients were older than 60. Additionally, the cohort was divided based on smoking history, with 63 smokers and 65 non-smokers. The inclusion criteria: (1) postoperative pathology verify as MIA following pulmonary lobectomy or segmentectomy, (2) complete thin-slice CT images available preoperatively, (3) EGFR gene detection conducted postoperatively, (4) absence of other space-occupying lesions before surgery, and (5) no anti-tumor treatment before surgery. The exclusion criteria: (1) multiple lung lesions, (2) patients who had received treatment before surgery, and (3) patients whose pathology revealed other types of space-occupying lesions.

Equipment and reagents

Philips 64-slice spiral CT machine (Netherlands Philips); Auantitative real-time PCR (Switzerland Roche Cobas Z 480); The EGFR gene detection kit (Switzerland Roche).

CT examination method

Preoperative CT scans were using a Philips Brilliance 64-slice spiral CT scanner, 5 mm slice thickness, with reconstruction settings adjusted to a slice thickness of 1 mm. Set 120 kV of the tube voltage and set current between 120 and 380 mA.

CT image analysis

Two radiologists own five years of experience, independent analyzed, diagnosed, and recorded the various CT features of pulmonary nodules without knowledge of the patients' gene mutation statuses. The average of the two radiologists' readings used as the final value for measured values. In cases of disagreement regarding a lesion, a consensus reached through discussion. The CT features analyzed included the average diameter of nodules, pleural indentation sign, peripheral fibrosis, spiculation sign, tumor-lung interface, lobulation sign, vacuole sign, vascular convergence sign, density, air bronchogram, peripheral emphysema, and morphology. Partial CT signs of MIA illustrated in figure 1.

Pathological examination method

Surgically excised specimens were sent to the pathology laboratory, where experienced technicians soak the specimens in a 10% neutral formalin solution (approval number: Jiangsu Drug Administration (quasi) word 2016 No. 20160001 China) for fixation,

dehydration, transparency, embedding, sectioning, and processing with the use of hematoxylin-eosin (HE) staining (Beijing Yili Fine Chemicals Co., LTD. China). The diagnosis of MIA was verified by two pathologists after consultation, on the basis of the 2021 pathological criteria for lung adenocarcinoma⁽¹⁹⁾. Pathological images of MIA illustrated in figure 2.

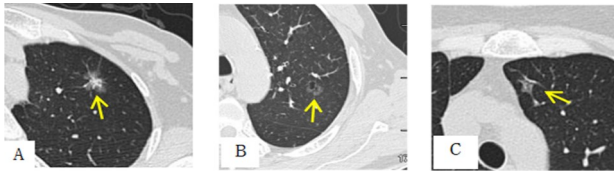


Figure 1. Legend of CT signs of minimally invasive adenocarcinoma (MIA) with EGFR gene mutation. **A:** CT scan of a 54-year-old woman showing a mixed ground-glass opacity (GGO) nodule in the upper lobe of the left lung, measuring approximately 1.5 cm in diameter, with a visible spiculation sign (indicated by the arrow). **B:** CT scan of a 48-year-old man depicting a GGO nodule in the upper lobe of the left lung, measuring approximately 1.0 cm in diameter, with a visible vacuole sign (indicated by the arrow). **C:** CT scan of a 68-year-old woman showing a GGO nodule in the upper lobe of the left lung, measuring approximately 1.1 cm in diameter, with a visible vascular convergence sign (indicated by the arrow).
Abbreviations: GGO, ground-glass opacity.

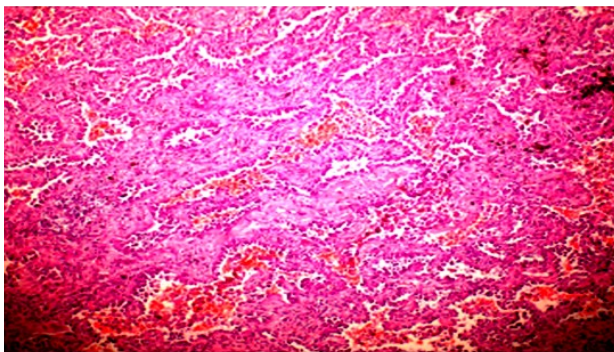


Figure 2. Pathological image of minimally invasive lung adenocarcinoma, stained with hematoxylin and eosin (HE, x10).

Gene detection methods

DNA was extracted from formaldehyde-fixed, paraffin-embedded tissue sections using Roche FFPE Tissue Kit (Switzerland Roche) according to the manufacturer's instructions. PCR analysis of The EGFR gene detection kit (Switzerland Roche) was performed using quantitative real-time PCR (Switzerland Roche Cobas Z 480) and the results were interpreted according to the manufacturer's instructions. With reference to the CAP / IASLC / AMP guideline^[20], molecular mutations in the EGFR gene were defined as mutations in EGFR exons 18,19,20,21, and other types of EGFR mutations were defined as wild-type EGFR.

The detection steps are as follows: (1) Making amplification agent: the reaction mixture thawed at room temperature, and the thawed reagent, mixed enzyme solution and purified water, followed by centrifugation for 10s, the mixture was made and

packaged in each PCR reaction tube, and then added the sample. (2) Sample addition: 2 μ L DNA sample, EGFR negative and positive quality control were successively added to the PCR reaction tube, centrifuged for 10s, and then amplified. (3) PCR amplification: First, the reaction was carried out at 95 $^{\circ}$ C for 5min, cycle once. Second, the reaction was carried out at 95 $^{\circ}$ C, 60 $^{\circ}$ C and 72 $^{\circ}$ C with 30s, and the cycle was 32 times. In the third stage, the cells were incubated at 95 $^{\circ}$ C, 60 $^{\circ}$ C and 72 $^{\circ}$ C for 25s and 10 cycles, respectively. (4) Read the results.

Because this study is a retrospective analysis, the classification of cases is compared according to whether there is the EGFR gene mutation, without detailed analysis of which mutation site and the gene detection in this study is selected to use the kit provided by Roche. It gives the test results (mutation type) directly by itself. These cases were not verified by gene sequencing.

Statistical analysis

Data were used SPSS version 22.0. The clinical data and CT features of the cases categorized into a mutation group and a wild-type group. The Chi-square with Fisher's exact tests were used to assess statistical significance. Binary logistic regression analysis was guided on statistically significant variables to develop a predictive model for EGFR gene mutations in MIA.

RESULTS

Clinical data and EGFR gene mutation status

Among the 118 cases of minimally invasive lung adenocarcinoma, 69 by mutation group, 49 by the wild-type group. This cohort consisted have 67 females (62.3%) and 51 males (37.7%), with no significant in gender ($P>0.05$). Although the mutation rate was relatively high (66.7%) among the 70 patients more than 60 years, the difference was not significant ($P>0.05$). Patients were also divided into smokers ($n=63$) and non-smokers ($n=65$), no significant difference with smoking history ($P>0.05$) (table 1).

Table 1. Comparison of clinical data between EGFR mutation group and wild-type group in patients with (MIA).

| Analytical factor | Cases (n=118) | Mutation group (n=69) | Wild group (n=49) | χ^2 | P |
|------------------------|---------------|-----------------------|-------------------|----------|-------|
| Age (year) | | | | 3.714 | 0.054 |
| <60 | 48 | 23(33.3%) | 25(51%) | | |
| ≥ 60 | 70 | 46(66.7%) | 24(49%) | | |
| Gender | | | | 2.078 | 0.149 |
| Man | 51 | 26(37.7%) | 25(51%) | | |
| Woman | 67 | 43(62.3%) | 24(49%) | | |
| Smoking history | | | | 2.482 | 0.115 |
| Yes | 63 | 35(50.7%) | 32(65.3%) | | |
| No | 65 | 34(49.3%) | 17(34.7%) | | |

NOTE: MIA: Minimally invasive adenocarcinoma.

CT features and EGFR mutation status

The analysis of CT features with the EGFR gene

mutation status in MIA revealed no statistically significant differences in the average diameter for nodules, density, morphology, lobulation sign, pleural indentation sign, air bronchogram, tumor-lung interface, peripheral emphysema, and peripheral fibrosis (P>0.05). Between the two groups regarding spiculation sign, vacuole and vascular convergence sign had statistically significant (P<0.05). Partial CT signs with pathological images of MIA illustrated in table 2.

Table 2. Comparison of CT characteristics and EGFR gene mutation status in MIA.

| CT features | All patients (n=118) | The EGFR gene mutation status | | Inspection value | p-Value |
|----------------------------------|----------------------|-------------------------------|-------------------|------------------|--------------------|
| | | Mutation group (n=69) | Wild group (n=49) | | |
| Average diameter | | | | - | 0.549 [#] |
| ≤10mm | 36 | 21(30.4%) | 15(30.6%) | | |
| ≤20mm | 68 | 38(55.1%) | 30(61.2%) | | |
| ≤30mm | 14 | 10(14.5%) | 4(8.2%) | | |
| Spiculation sign | | | | 5.812* | 0.016 |
| Yes | 65 | 45(65.2%) | 21(42.9%) | | |
| No | 53 | 24(34.8%) | 28(57.1%) | | |
| Vacuola sign | | | | 4.621* | 0.032 |
| Yes | 62 | 42(60.9%) | 20(40.8%) | | |
| No | 56 | 27(39.1%) | 29(59.2%) | | |
| Density | | | | 3.242* | 0.072 |
| GGO | 68 | 35(50.7%) | 33(67.3%) | | |
| Mixed GGO | 50 | 34(49.3%) | 16(32.7%) | | |
| Lobulation sign | | | | 6.642* | 0.056 |
| Yes | 39 | 18(26.1%) | 21(42.9%) | | |
| No | 79 | 51(73.9%) | 28(57.1%) | | |
| Morphology | | | | 0.625* | 0.429 |
| Regular | 82 | 46(66.7%) | 36(73.5%) | | |
| Irregular | 36 | 23(33.3%) | 13(26.5%) | | |
| Pleural indentation sign | | | | 0.320* | 0.571 |
| Yes | 47 | 26(37.7%) | 21(42.9%) | | |
| No | 71 | 43(62.3%) | 28(57.1%) | | |
| Air bronchial sign | | | | 1.624* | 0.202 |
| Yes | 45 | 23(33.3%) | 22(44.9%) | | |
| No | 73 | 46(66.7%) | 27(55.1%) | | |
| Tumor-lung interface | | | | 0.285* | 0.593 |
| distinct | 64 | 36(52.2%) | 28(57.1%) | | |
| indistinct | 54 | 33(47.8%) | 21(42.9%) | | |
| Vascular convergence sign | | | | 4.902* | 0.027 |
| Yes | 78 | 40(58%) | 38(77.6%) | | |
| No | 40 | 29(42%) | 11(22.4%) | | |
| Peripheral emphysema | | | | - | 0.091 [#] |
| Yes | 10 | 3(4.3%) | 7(14.3%) | | |
| No | 98 | 66(95.7%) | 42(85.7%) | | |
| Peripheral fibrosis | | | | 0.438 | 0.508 [#] |
| Yes | 30 | 16(23.2%) | 14(28.6%) | | |
| No | 88 | 53(76.8%) | 35(71.4%) | | |

Note: 1 # represents the Fisher exact probability test; 2 * represents the Chi-square test; GGO: Ground Glass Opacity; MIA: Minimally Invasive Adenocarcinoma.

Chi-square tests revealed that the spiculation sign and vascular convergence sign in MIA were statistically (P<0.05). These signs were included in a binary logistic regression analysis to make up a predictive model for EGFR in MIA. This analysis demonstrated that vascular convergence sign and spiculation sign are independent risk factors for predicting EGFR gene mutations. ROC curves were generated based on the spiculation and vascular convergence signs. AUC for spiculation sign is 0.634, with sensitivity of 85.02% and a specificity of 35.21%. The AUC for the vascular convergence sign was 0.735, with a sensitivity of 84.48% and a specificity of 37.56% (table 3, figure 3).

Table 3. Results of logistic regression analysis for minimally invasive adenocarcinoma (MIA).

| Variable | B | S.E. | Wald | P | OR | 95%CI |
|----------------------------------|--------|-------|-------|-------|-------|-------------|
| vascular convergence sign | 1.168 | 0.729 | 4.353 | 0.026 | 2.262 | 1.030,4.547 |
| vacuole sign | -0.443 | 0.965 | 0.529 | 0.521 | 0.410 | 0.339,4.212 |
| spiculation sign | 1.423 | 0.995 | 2.092 | 0.017 | 1.498 | 0.247,4.903 |

NOTE: MIA: Minimally Invasive Adenocarcinoma. B: The regression coefficient reflects the influence of the independent variable on the dependent variable; S.E.: The standard error reflects the estimation accuracy of the regression coefficient, and the smaller the standard error, the more accurate the estimation of the regression coefficient; Wald: The Wald statistic was used to test whether the regression coefficients were significantly not 0; P: Reflecting the significant level of this test, with p<005, this independent variable was considered to have a significant influence on the dependent variable; OR: The image degree index reflecting the variable for the classification outcome.

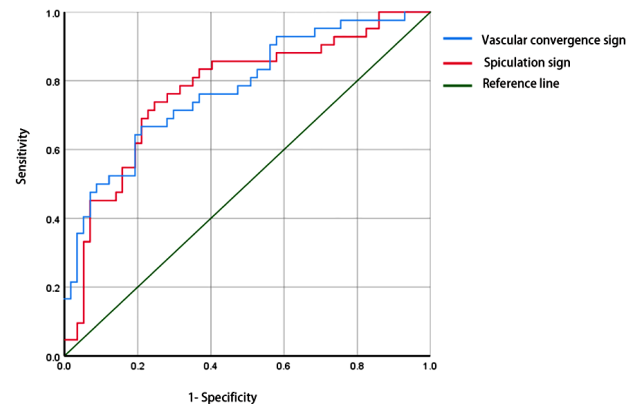


Figure 3. Ensure that the receiver operating characteristic curve (ROC) analysis of the spiculation sign and vascular convergence sign in predicting minimally invasive adenocarcinoma (MIA) is of high quality.

DISCUSSION

The pathogenesis of lung adenocarcinoma is complex, involving many factors such as genetics, chronic lung infection and environmental pollution. Its malignant degree is high. If timely screening and treatment cannot done, tumor invasion and distant metastasis can appear with the progression of the disease, and the mortality rate is high (21). The rapid advancements and widespread application of imaging technologies have greatly improved the detection rate of early-stage lung cancer. Imaging techniques can partially reflect the molecular characteristics of tumors, and predicting EGFR gene mutation status through imaging examinations has become an

important research field⁽²²⁾. However, the relationship between imaging characteristics with the EGFR gene mutations of lung adenocarcinoma remains in the early stages of research, leading to inconsistent conclusions across studies^(15, 17, 18).

Regarding clinical characteristics, some studies suggest that models predicting EGFR mutations based on age, gender, and smoking history alone are less accurate^(23, 24). Consequently, there are limitations to using these factors exclusively to predict EGFR gene mutations, which aligns with the findings of this study. However, many studies have demonstrated that young, non-smoking women are more likely own the EGFR mutable gene in lung adenocarcinoma^(16, 25). These discrepancies could be attributed to differences in clinical characteristics, regional variations, and racial differences among the study populations.

The study pointed out that the size of the lesion was connected with the pathological process. Most solid lesions greater than 3cm were invasive lung adenocarcinoma, while pure ground glass nodules less than 1.5cm in diameter had a low incidence of invasive lung adenocarcinoma⁽²⁶⁾. In terms of lesion diameter from CT quantitative analysis, this study is consistent with most reports, showing no correlation between lesion size and EGFR gene mutation status^(27, 28). However, Zhang *et al.* observed that as the average lesion diameter increases, indicating a positive correlation between lesion size and EGFR mutations⁽²⁹⁾. This study had microinvasive lung adenocarcinoma lesions less than 3cm long, which differs from studies focusing on invasive lung adenocarcinoma, where most lesions exceed 3cm. This difference in case selection may account for the divergent conclusions. Regarding the pleural indentation sign on CT, this study agrees with Song's findings, which concluded that there are no relationship EGFR mutations with pleural indentation⁽³⁰⁾. Pleural indentation is primarily caused by reactive fibroplasia or scar formation within the lesion, pulling the local pleura and forming a cable-like shadow. It is commonly associated with pleural invasion, indicating a more aggressive tumor with a poorer prognosis^(31,32). In contrast, NIE *et al.* found that pleural indentation was more prevalent in patients with EGFR mutations, suggesting it may have some predictive value⁽³³⁾. However, their study included more cases of invasive lung adenocarcinoma, which could explain the difference in findings, as this study focused on microinvasive lung adenocarcinoma with a lower malignancy rate. Most studies suggest that signs such as vacuolation, spiculation, and vascular convergence correlated with EGFR gene mutations^(34, 35). Huo Jiwen *et al.* identified spiculation and vascular convergence as independent predictors of EGFR mutations in the study of 803 cases, consistent with these results⁽³⁴⁾. However, Juna *et al.* found no correlation between these CT signs and EGFR gene expression⁽³⁶⁾. Their study, which included 354 lung adenocarcinoma

lesions, showed that invasive lung adenocarcinoma was more prone to EGFR mutations, further supporting the relationship between EGFR mutations and tumor infiltration⁽³⁷⁾. These differences in pathological results and case selections between studies may contribute to the varying findings. This study did not identify correlations between other CT characteristics and EGFR mutations, possibly due to subjective differences, staging variations, ethnic differences, and researchers' judgment in evaluating morphological signs.

The main limitations of this study were the insufficient quantitative analysis of lesions. Future research should involve larger sample sizes, incorporate additional CT features and imaging omics data, and utilize digital image processing technology to analyze the morphology of lung adenocarcinoma lesions quantitatively. This approach will further explore the relationship between gene mutations and imaging features.

CONCLUSION

CT imaging of microinvasive lung adenocarcinoma revealed a high rate of EGFR gene mutations in cases with spiculation, vacuolation, and vascular convergence signs. Spiculation and vascular convergence signs identified as independent risk factors for predicting EGFR gene mutations.

Acknowledgments: The authors would like to sincerely thank all the researchers and organizations that contributed to this study.

Funding: No funding supported this study.

Conflicts of Interest: All authors unanimously declare no conflict of interest in this study.

Ethical Consideration: This retrospective study was approved by the research Ethics Committee of Tangshan Gongren Hospital with the number GRYY-LL-2018-48 at 26th Nov 2018.

Author Contribution: L.P.Z. and L.M.C.; conceived and designed the study. H.Z. and J.T.W.; conducted the literature search and data collection. L.L.S. analyzed the data. L.P.Z. and L.M.C. wrote the paper. L.P.Z. and X.Y.Y.; reviewed and edited the manuscript. All authors read and approved the final manuscript.

REFERENCES

1. Sung H, Ferlay J, Siegel RL, *et al.* (2021) Global cancer statistics 2020: GLOBOCAN estimates of incidence and mortality worldwide for 36 cancers in 185 countries. *CA: A Cancer Journal for Clinicians*, **71**(3): 209-249. DOI:10.3322/caac.21660
2. Antonicelli A, Cafarotti S, Indini A, *et al.* (2013) EGFR-targeted therapy for non-small cell lung cancer: focus on EGFR oncogenic mutation. *Int J Med Sci*, **10**(3): 320-330. DOI:10.7150/ijms.4609
3. Travis WD, Brambilla E, Noguchi M, *et al.* (2011) International Association for the Study of Lung Cancer/American Thoracic Society/European Respiratory Society: international multidisciplinary classification of lung adenocarcinoma: executive summary. *Proc Am Thorac Soc*, **8**(5): 381-385. DOI: 10.1513/pats.201107-042ST

4. Gao JW, Rizzo S, Ma LH, *et al.* (2017) Pulmonary ground-glass opacity: computed tomography features, histopathology and molecular pathology. *Transl Lung Cancer Res*, **6**(1): 68-75. DOI:10.21037/tlcr.2017.01.02
5. Yotsukura M, Asamura H, Motoi N, *et al.* (2021) Long-term prognosis of patients with resected adenocarcinoma in situ and minimally invasive adenocarcinoma of the lung. *J Thorac Oncol*, **16**(8): 1312-1320. DOI:10.1016/j.jtho.2021.04.007
6. Hasegawa M, Sakai F, Ishikawa R, *et al.* (2016) CT features of epidermal growth factor receptor-mutated of the lung: comparison with nonmutated adenocarcinoma. *J Thorac Oncol*, **11**(6): 819-26. DOI:10.1016/j.jtho.2016.02.010
7. Pinilla-Macua I, Grassart A, Duvvuri U, *et al.* (2017) Sorkin A. EGF receptor signaling, phosphorylation, ubiquitylation and endocytosis in tumors in vivo. *Elife*, **21**(6): e31993. DOI: 10.7554/eLife.31993
8. Levantini E, Maroni G, Del Re M, *et al.* (2022) EGFR signaling pathway as a therapeutic target in human cancers. *Seminars in Cancer Biology*, **85**: 253-275. DOI:10.1016/j.semcancer.2022.04.002
9. Fei YC, Zhou LM, Lu DL (2021) Research progress of EGFR extracellular domain mutation in non-small cell lung cancer. *Chinese Journal of New Drugs*, **30**(17): 1579-1583. DOI:10.3969/j.issn.1003-3734.2021.17.008
10. Colombino M, Paliogiannis P, Cossu A, *et al.* (2019) EGFR, KRAS, BRAF, ALK, and cMET genetic alterations in 1440 Sardinian patients with lung adenocarcinoma. *BMC Pulmonary Medicine*, **19**(1): 209. DOI:10.1186/s12890-019-0964-x
11. Zhou L and Chen Z (2021) Successful treatment of a patient with an EGFR mutated pulmonary adenocarcinoma and a history of uremia with erlotinib after gefitinib-induced kidney dysfunction: a case report. *International Journal of Radiation Research*, **19**(3): 749-753. DOI: 10.29252/ijrr.19.3.749
12. Shi Z, Song CE, Shi RF, *et al.* (2017) CT and Clinical features associated with epidermal growth factor receptor mutation of exon 19 in lung adenocarcinoma. *Journal of Clinical Radiology*, **36**(04): 490-494. DOI:10.13437/j.cnki.jcr.2017.04.012.
13. Zhang Y, Yao Y, Xu Y, *et al.* (2021) Pan-cancer circulating tumor DNA detection in over 10,000 Chinese patients. *Nat Commun*, **12**(1): 11. DOI:10.1038/s41467-020-20162-8.
14. Jiang X, Miao L, Yang L, *et al.* (2024) Advances in diagnostic imaging of small cell lung cancer. *Chinese Journal of General Practice*, **22**(02): 296-300. DOI:10.16766/j.cnki.issn.1674-4152.003388
15. Han X, Fan J, Li Y, *et al.* (2021) Value of CT features for predicting EGFR mutations and ALK positivity in patients with lung adenocarcinoma. *Sci Rep*, **11**(1): 5679. DOI:10.1038/s41598-021-83646-7
- Han X, Fan J, Gu J, *et al.* (2020) CT features associated with EGFR mutations and ALK positivity in patients with multiple primary lung adenocarcinomas. *Cancer Imaging*, **20**(1): 51. DOI:10.1186/s40644-020-00330-1
17. Zhang G, Zhao Z, Cao Y, *et al.* (2021) Relationship between epidermal growth factor receptor mutations and CT features in patients with lung adenocarcinoma. *Clin Radiol*, **76**(6): 473. DOI:10.1016/j.crad.2021.02.012.
18. Cheng L, Sun W, Peng DG, *et al.* (2024) Research progress on the relationship between CT manifestations of ground-glass nodules in lung adenocarcinoma and common gene mutations. *Clinical Journal of Medical Officers*, **52**(04): 437-440. DOI:10.16680/j.1671-3826.2024.04.29
19. Nicholson AG, Tsao MS, Beasley MB, *et al.* (2022) The 2021 WHO classification of lung tumors: impact of advances since 2015. *Journal of Thoracic Oncology*, **17**(3): 362-387. DOI:10.1016/j.jtho.2021.11.003
20. Rekhtman N, Leighl NB, Somerfield MR (2015) Molecular testing for selection of patients with lung cancer for epidermal growth factor receptor and anaplastic lymphoma kinase tyrosine kinase inhibitors: American society of clinical oncology endorsement of the college of American pathologists/international association for the study of lung cancer/association for molecular pathology guideline. *J Oncol Pract*, **11**: 135-136. DOI:10.1200/JOP.2014.002303
21. El-Deek S E, Abdel-Ghany S M, Hana R S, *et al.* (2021) Genetic polymorphism of lysyl oxidase, glutathione S-transferase M1, glutathione-S-transferase T1, and glutathione S-transferase P1 genes as risk factors for lung cancer in Egyptian patients. *Molecular Biology Reports*, **48**(5): 4221-4232. DOI:10.1007/s11033-021-06436-4
22. Usuda K, Sagawa M, Motono N, *et al.* (2014) Relationships between EGFR mutation status of lung cancer and preoperative factors—are they predictive? *Asian Pacific Journal of Cancer Prevention*, **15**(2): 657-662. DOI:10.7314/apjcp.2014.15.2.657
23. Wang S, Shi J, Ye Z, *et al.* (2019) Predicting EGFR mutation status in lung adenocarcinoma on computed tomography image using deep learning. *European Respiratory Journal*, **53**(3):1800986. DOI:10.1183/13993003.00986-2018
24. Girard N, Sima CS, Jackman DM, *et al.* (2021) Nomogram to predict the presence of EGFR activating mutation in lung adenocarcinoma. *European Respiratory Journal*, **39**(2): 366e72. DOI:10.3969/j.issn.1671-4695.2022.04.007
25. Yang Y, Yang Y, Zhou X, *et al.* (2015) EGFR L858R mutation is associated with lung adenocarcinoma patients with dominant ground-glass opacity. *Lung Cancer*, **87**(3): 272-277. DOI:10.1016/j.lungcan.2014.12.016
26. Duan L, Shan W, Guo L, *et al.* (2022) Correlation in high resolution computed tomography signs with pathological subtype and differentiation degree of lung adenocarcinoma. *International Journal of Radiation Research*, **20**(3): 679-685. DOI: 10.52547/ijrr.20.3.23
27. Sun F, Xi J, Zhan C, *et al.* (2018) Ground glass opacities: imaging, pathology, and gene mutations. *Journal of Thoracic and Cardiovascular Surgery*, **156**(2): 808-813. DOI:10.1016/j.jtcvs.2018.02.110
28. Zhang Q, Zhang Y, Xiong Y, *et al.* (2022) Analysis of CT features of EGFR mutant lung adenocarcinoma. *Journal of Clinical Radiology*, **41**(06): 1019-1024. DOI:10.13437/j.cnki.jcr.2022.06.004
29. Zhang LB, Shen LL, Wang B, *et al.* (2021) Correlation between epidermal growth factor receptor mutation and histologic subtypes or characteristics of computed tomography findings in patients with pulmonary adenocarcinoma. *Academic Journal of Chinese PLA Medical School*, **42**(10): 1035-1039+1057. DOI:10.3969/j.issn.2095-5227.2021.10.006
30. Song B, Min XH, Chen W, *et al.* (2019) Clinical analysis of the association between EGFR and CT scan images in early-stage lung cancer with pulmonary ground glass nodules. *The Practical Journal of Cancer*, **34**(2): 215-218+234. DOI:10.3969/j.issn.1001-5930.2019.02.011
31. Cai Y, Chen T, Zhang S (2021) Correlation exploration among CT imaging, pathology, and genotype of pulmonary ground-glass opacity. *Journal of Cellular and Molecular Medicine*, **27**(14): 2021-2031. DOI:10.1111/jcmm.17797
32. Zhang H, Cai W, Wang Y, *et al.* (2019) CT and clinical characteristics that predict the risk of EGFR mutation in non-small cell lung cancer: a systematic review and meta-analysis. *International Journal of Clinical Oncology*, **24**(6): 649-659. DOI:10.1007/s10147-019-01403-3
33. Nie Y, Liu H, Tan X, *et al.* (2019) Correlation between high-resolution computed tomography lung nodule characteristics and EGFR mutation in lung adenocarcinomas. *Oncotargets and Therapy*, **12**: 519-526. DOI:10.2147/OTT.S184217
34. Huo JW, Li Q, Luo T, *et al.* (2021) The value of clinical and CT features in predicting EGFR mutation of lung adenocarcinoma. *Radiologic Practice*, **36**(11): 1375-1381. DOI:10.13609/j.cnki.1000-0313.2021.11.008
35. Zhang G, Zhang J, Cao Y, *et al.* (2021) Nomogram based on preoperative CT imaging predicts the EGFR mutation status in lung adenocarcinoma. *Translational Oncology*, **14**(1): 100954. DOI:10.1016/j.tranon.2020.100954
36. Zhu N, Zhang CY, Ma N, *et al.* (2021) Correlation between CT signs of pulmonary adenocarcinoma appearing as ground-glass nodule and epidermal growth factor receptor gene expression. *Chinese Journal of Medical Imaging*, **29**(11): 1095-1099. DOI:10.3969/j.issn.1005-5185.2021.11.009
37. Lu Q, Ma Y, An Z, *et al.* (2018) Epidermal growth factor receptor mutation accelerates radiographic progression in lung adenocarcinoma presented as a solitary ground-glass opacity. *Journal of Thoracic Disease*, **10**(11): 6030-6039. DOI:10.21037/jtd.2018.10.19